

Rounded Hartley Transform: A Quasi-involution*

R. J. Cintra[†] H. M. de Oliveira[‡] C. O. Cintra[§]

Abstract

A new multiplication-free transform derived from DHT is introduced: the RHT. Investigations on the properties of the RHT led us to the concept of weak-inversion. Using new constructs, we show that RHT is not involutorial like the DHT, but exhibits quasi-involutional property, a new definition derived from the periodicity of matrices. Thus instead of using the actual inverse transform, the RHT is viewed as an involutorial transform, allowing the use of direct (multiplication-free) to evaluate the inverse. A fast algorithm to compute RHT is presented. This algorithm show embedded properties. We also extended RHT to the two-dimensional case. This permitted us to perform a preliminary analysis on the effects of RHT on images. Despite of some SNR loss, RHT can be very interesting for applications involving image monitoring associated to decision making, such as military applications or medical imaging.

Keywords

DCT Approximation, Fast algorithms, Image compression

1 Introduction

Discrete transforms have a significant role in digital signal processing. A relevant example is the discrete Hartley transform (DHT), which offers many advantages over the more popular discrete Fourier transform. To cite major advantages, (i) DHT is a real-valued transform (no complex arithmetic is needed), (ii) it possesses same formula for forward and inverse transform, (iii) it has a computational equivalence to DFT [10], (iv) DHT shows high symmetry, which is desirable from the implementation point-of-view, and (v) it is mathematically elegant. These characteristics have motivated a lot of research to promote the use of DHT instead of DFT. Thus DHT has hit many applications such as spectral analysis, convolution computation, adaptive filters, interpolation, communication systems and medical imaging [12]. A representative reference list with the literature about the Hartley transform is found in [11].

Another important area of signal processing concerns with the minimal complexity methods. The class of multiplication-free discrete transforms, such as Walsh/Hadamard transform, has attracted much interest, since those transforms provide low computational complexity. The multiplication-free paradigm was adopted by Reed *et alii* in the definition of the arithmetic Fourier transform [13]. Recently an algorithm of this kind was proposed: the arithmetic Hartley transform [5]. An interesting approach was done by Bhatnagar: using Ramanujan numbers, another multiplication-free transform was invented [1]. Approximation procedures are also being taken in consideration. In a recent paper [8], Dee-Jeoti proposed the approximate fast Hartley transform, though multiplicative complexity is not null.

Seeking for new procedures with the multiplication-free motto in mind, we introduced in this paper a new transformation: the rounded Hartley transform (RHT), a transform with zero multiplicative complexity. Figure 1 places the RHT among other transforms.

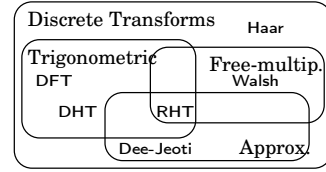


Figure 1: Discrete transforms and some of their classes. Rounded Hartley transform is placed in the intersection of many classes.

In section 2 and 3, we define the RHT and set the theoretical background to new concepts: quasi-equivalence, quasi-involution and weak-inversion, with simulation results. Section 4 brings a first approach to a fast algorithm for RHT, using the theoretical background found in [7]. We explored a naive example, 16-RHT, and derived arithmetic complexity bounds. Subsequently in section 5, the two-dimensional case was analyzed by introducing the 2-D RHT. The effects of 2-D RHT on standard classical images were investigated, particularly peak signal-noise ratio. We ended this paper establishing a connection between the new RHT and the Walsh/Hadamard transform.

2 The Rounded Hartley Transform

Let \mathbf{v} be an n -dimensional vector with real elements. The discrete Hartley transform establishes a pair of signal vectors $\mathbf{v} \xrightarrow{\mathcal{H}} \mathbf{V}$, where the elements of \mathbf{V} are defined by

$$V_k \triangleq \sum_{i=0}^{n-1} v_i \operatorname{cas}\left(\frac{2\pi ik}{n}\right), \quad k = 0, 1, \dots, n-1, \quad (1)$$

where $\operatorname{cas}(x) \triangleq \cos(x) + \sin(x)$. This transform leads to the definition of Hartley matrix \mathbf{H} , which elements are on the form $h_{i,k} = \operatorname{cas}\left(\frac{2\pi ik}{n}\right)$.

The roundoff of a matrix is obtained by rounding off its elements. Thus the rounded Hartley matrix elements $h_{i,k}$ are defined by

$$h_{i,k} \triangleq \underbrace{\operatorname{cas}\left(\frac{2\pi ik}{n}\right)}_{h_{i,k}}, \quad i, k = 0, 1, \dots, N-1, \quad (2)$$

*Manuscript originally published in 2002 at the International Telecommunications Symposium. Readers are encouraged to access newer results at <https://arxiv.org/abs/2007.02232>.

[†]R J Cintra is with the Signal Processing Group, Universidade Federal de Pernambuco, Recife, Brazil. E-mail: rjds@de.ufpe.br

[‡]H. M. de Oliveira is with the Signal Processing Group, Universidade Federal de Pernambuco, Recife, Brazil. E-mail: hmo@de.ufpe.br

[§]C. O. Cintra was with the Department of Physics and Mathematics, Rural Federal University of Pernambuco, Recife, Brazil.

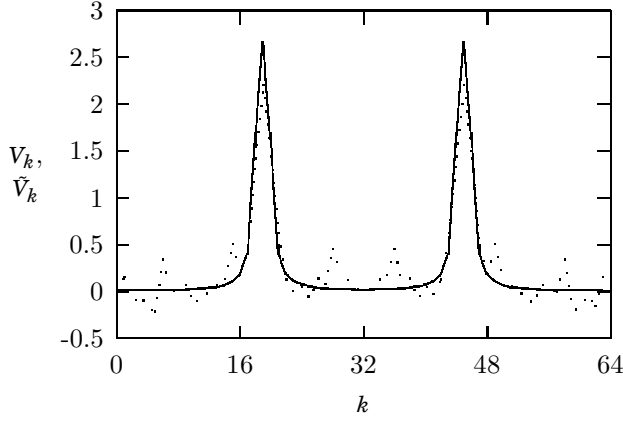


Figure 2: A Simple example. Hartley spectrum evaluated by discrete Hartley transform \mathbf{V} (filled line —) and rounded Hartley transform $\hat{\mathbf{V}}$ (dotted line \cdots) of a vector \mathbf{v} with 64 samples of function $f(x) = \cos(90\pi x)(x - \frac{1}{2})^2$, $0 \leq x \leq 1$.

where $[\cdot]$ denotes the nearest integer function. For the sake of notation, let us denote the rounded Hartley matrix by \mathbf{H} .

It is easy to see that the elements $h_{i,k}$ belong to $\{-1, 0, 1\}$, since $|\text{cas}(x)| \leq \sqrt{2}$. Consequently, the rounded Hartley transform can be implemented using only additions, regardless the block-length. Rounded Hartley transform is a multiplication-free transform, which can be very attractive from the practical point of view.

The first questions to be answered are: (i) Is the spectrum derived from RHT a good estimation of the (true) Hartley spectrum? (ii) Is there an inverse Hartley transform?

To begin with, we investigated the DHT and the RHT spectra for a few simple signals (HT has real-valued components). Figure 2 shows both spectra for the signal $f(x) = \cos(90\pi x)(x - \frac{1}{2})^2$ sampled by 64 points. A pretty good agreement was observed. A careful analysis of the error, or at least an upper bound, is currently being investigated.

3 Involution and Quasi-involution

In order to gain some insight on rounded Hartley transforms, intensity diagrams were generated. The value $h_{i,k}$ of each element of \mathbf{H}_n is converted into a gray-scale colormap and the matrix \mathbf{H}_n is then represented by a square with n^2 pixels. Some interesting patterns derived from RHT are show in Figure 3.

To keep rigorous with Hartley-Bracewell definition of the Hartley transform, in this section, the Hartley matrix \mathbf{H}_n and the rounded Hartley transform \mathbf{H}_n are scaled by $1/\sqrt{n}$. Without any kind of conceptual loss, this scaling does not interfere with the results hereafter derived and brings a greater elegance and harmony to the following constructs.

One of the most appealing properties of the classical DHT is the fact that discrete Hartley matrix \mathbf{H}_n is an involution, i.e., $\mathbf{H}_n^{-1} = \mathbf{H}_n$ (self-inverse). However, after the round operation, $\text{cas}(\cdot)$ kernel loses this characteristic and RHT is not an involution, since $\mathbf{H}_n^{-1} \neq \mathbf{H}_n$.

We found out by explicit computation that the inverse of \mathbf{H}_n does exist for order $n \leq 1024$. Unfortunately \mathbf{H}_n^{-1} is not as interesting as \mathbf{H}_n , since it is computationally more intensive. This fact was the key point that led us to a greater concern on inverse matrices. We are particularly interested in finding out matrices which have the properties of (i) being *almost* the inverse of a given matrix and (ii)

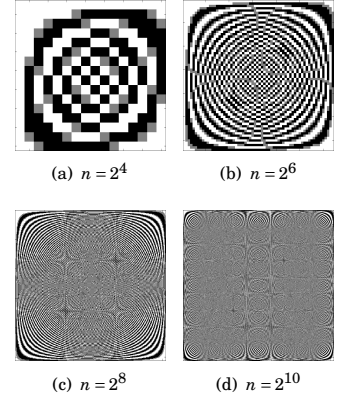


Figure 3: Image patterns derived from rounded Hartley matrix for orders $n = 16, 64, 256, 1024$. Each matrix \mathbf{H} is converted into intensity diagrams by representing their elements in a gray scale. Remark the presence of embedding patterns.

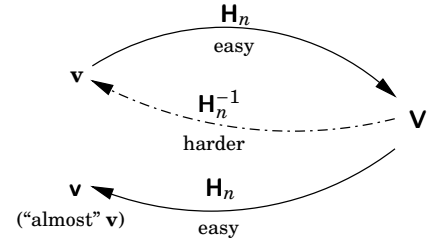


Figure 4: Concept of weak-inversion. This diagram show the main idea behind our work. We are concerned with matrices that “almost” invert. Filled arrows represent low computational complexity, while the dashed one stands for a higher computational complexity.

being computationally more interesting than the actual inverse. That is, given a matrix \mathbf{A} we are looking for a matrix $\tilde{\mathbf{A}}$, such as:

$$\mathbf{A} \cdot \tilde{\mathbf{A}} \approx \mathbf{I}_n. \quad (3)$$

This is what we called a *weak-inverse*.

After further examination on \mathbf{H}_n^{-1} , we observed that it resembles \mathbf{H}_n itself. In fact, \mathbf{H}_n^{-1} is *almost* \mathbf{H}_n . Since \mathbf{H}_n is defined from \mathbf{H}_n , we verify that \mathbf{H}_n is, in some sense, *almost* involutorial.

The qualitative idea was exposed, Figure 4 may elucidate it. Now it is time to imbue with some formalism this new concept and establish strict definitions for the weak-inverse.

3.1 Theory

Definition 1 (Matrix Period) The period of a matrix \mathbf{A} is the smallest positive integer k such that $\mathbf{A}^{k+1} = \mathbf{A}$. \square

For example, an idempotent transformation T satisfies $T^2 = T$, since it has period $k = 1$. An involution of a linear transformation can be defined as a transformation which has period $k = 2$.

Definition 2 The n -norm of a matrix \mathbf{A} is defined by

$$\bar{\mu}(\mathbf{A}) = \frac{\|\mathbf{A}\|}{n}, \quad (4)$$

where n is the order of \mathbf{A} and $\|\cdot\|$ represents Frobenius norm of a matrix:

$$\|\mathbf{A}\| = \left(\sum_{i=1}^n \sum_{j=1}^n |a_{i,j}|^2 \right)^{1/2},$$

where $a_{i,j}$ are the elements of matrix \mathbf{A} . \square

A family of matrices is defined as a sequence of matrices of increasing order, which are generated by some rule. A naive example is the identity family which is formed by all identity matrices:

$$\mathcal{J} = \{\mathbf{I}_1, \mathbf{I}_2, \mathbf{I}_3, \dots\}.$$

Another example is the Fourier matrix family:

$$\mathcal{F} = \{\mathbf{F}_1, \mathbf{F}_2, \mathbf{F}_3, \dots\}$$

where matrices \mathbf{F}_n have their elements defined according to

$$f_{i,k} = \exp\left(-j\frac{2\pi ik}{n}\right), \quad i, k = 0, \dots, n-1.$$

As a final example, the Hartley matrix family

$$\mathcal{H} = \{\mathbf{H}_1, \mathbf{H}_2, \mathbf{H}_3, \dots\}$$

is the sequence \mathbf{H}_n of matrices with elements defined by

$$h_{i,k} = \text{cas}\left(\frac{2\pi ik}{n}\right), \quad i, k = 0, \dots, n-1.$$

Definition 3 (Quasi-equivalence) Two families of matrices and \mathcal{B} are said to be quasi-equivalent at a level ϵ if and only if for any two matrices $\mathbf{A} \in \mathcal{A}$ and $\mathbf{B} \in \mathcal{B}$ of same order there exist a positive real number ϵ such as

$$\bar{\mu}(\mathbf{A} - \mathbf{B}) \leq \epsilon. \quad (5)$$

Consider a family of matrices $\mathcal{A} = \{\mathbf{A}_1, \mathbf{A}_2, \dots\}$. Let us denote \mathcal{A}_k the family which contains the matrices of \mathcal{A} raised to the k th power, i.e., $\mathcal{A}_k = \{\mathbf{A}_1^k, \mathbf{A}_2^k, \dots\}$.

Definition 4 (Quasi-periodicity) The quasi-period of a matrix $\mathbf{A}_i \in \mathcal{A}$ is the smallest positive integer k such that there exist a family of matrices $\mathcal{A}_k = \{\mathbf{A}_1^k, \mathbf{A}_2^k, \dots, \mathbf{A}_i^k, \dots\}$ which is quasi-equivalent to the identity family \mathcal{J} .

That is, for some ϵ , the following equation is satisfied

$$\bar{\mu}(\mathbf{A}_n^k - \mathbf{I}_n) \leq \epsilon, \quad \forall n. \quad (6)$$

The matrix \mathbf{A} is said to be quasi-periodic with quasi-period k . A consequence of this definition is stated in the following proposition.

Proposition 1 All matrices in a family have the same quasi-period.

Proof: Let $\mathcal{A} = \{\mathbf{A}_1, \mathbf{A}_2, \mathbf{A}_3, \dots\}$ be a family of matrices. Suppose that each matrix \mathbf{A}_i has a given quasi-period k_i . By Definition 4, if a matrix \mathbf{A}_n has quasi-period k_n , then there exists a family

$$\mathcal{A}_{k_n} = \{\mathbf{A}_1^{k_n}, \mathbf{A}_2^{k_n}, \dots, \mathbf{A}_n^{k_n}, \dots, \mathbf{A}_m^{k_n}, \dots\}$$

which is quasi-equivalent to the identity family \mathcal{J} . Now let another matrix \mathbf{A}_m with quasi-period k_m . Analogously, it implies that there exist a family

$$\mathcal{A}_{k_m} = \{\mathbf{A}_1^{k_m}, \mathbf{A}_2^{k_m}, \dots, \mathbf{A}_n^{k_m}, \dots, \mathbf{A}_m^{k_m}, \dots\}$$

which is quasi-equivalent to the identity family \mathcal{J} .

Since quasi-period is defined as the smallest integer for which the above conditions are satisfied, it yields that $k_n \leq k_m$ and $k_m \leq k_n$. Thus $k_n = k_m$. \square

After these theoretical background, we can formalize the concept of weak-inversion. A matrix $\tilde{\mathbf{A}}_n$ is a weak-inverse of \mathbf{A}_n if the family of matrices $\mathbf{A}_n \tilde{\mathbf{A}}_n$ is quasi-equivalent to the identity family, i.e.,

$$\bar{\mu}(\mathbf{A}_n \tilde{\mathbf{A}}_n - \mathbf{I}_n) \leq \epsilon \quad \forall n. \quad (7)$$

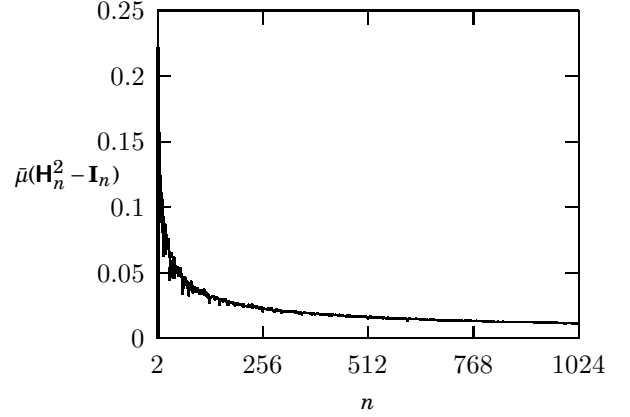


Figure 5: The n -norm of $(\mathbf{H}_n^2 - \mathbf{I}_n)$ for $n = 2, 3, \dots, 1024$.

3.2 The Weak-Inverse of Rounded Hartley Matrix

Now let us get back to the rounded Hartley matrix \mathbf{H}_n . Evaluating the n -norm of $\mathbf{H}_n^2 - \mathbf{I}_n$ for $n = 2, 3, \dots, 1024$, one can plot the graph depicted in Figure 5. After a data analysis of these points, we fitted them to a Freundlich model:

$$\bar{\mu}(\mathbf{H}_n^2 - \mathbf{I}_n) \approx an^b, \quad (8)$$

where $a \approx 0.35167$ and $b \approx -0.49324$.

These observations are the background needed to infer on the asymptotical behavior of $\bar{\mu}(\mathbf{H}_n^2 - \mathbf{I}_n)$ and state the following conjecture:

Conjecture 1

$$\lim_{n \rightarrow \infty} \bar{\mu}(\mathbf{H}_n^2 - \mathbf{I}_n) = 0. \quad (9)$$

An immediate consequence of this conjecture is that $\bar{\mu}(\mathbf{H}_n^2 - \mathbf{I}_n)$ is bounded and has its maximum value at $n = 3$ (see Figure 5). That is,

$$\bar{\mu}(\mathbf{H}_n^2 - \mathbf{I}_n) \leq \frac{2}{9}, \quad n = 2, 3, \dots$$

According to Equation 7, it comes to uses that \mathbf{H}_n is the weak-inverse of itself. Furthermore under conditions of Definition 4, we can state that rounded Hartley matrices are quasi-periodic and their quasi-period is two.

Definition 5 (Quasi-involution) A quasi-involution is a transform with quasi-period of 2. \square

3.3 General Comments

In this subsection, we state some initial observations about the rounded Hartley transform without further derivations or proofs.

3.3.1 Error

Since a weak-inverse is not precisely the inverse of a given matrix, this approach of retrieving data from a weak-inverse introduces some degradation, as expected. The RHT is given by $\mathbf{V} = \mathbf{H}_n \mathbf{v}$. We shall use $\mathbf{v} = \mathbf{H}_n \mathbf{V} = \mathbf{H}_n^2 \mathbf{v}$ to compute the inverse, instead of the exact inverse RHT $\mathbf{v} = \mathbf{H}_n^{-1} \mathbf{V}$. Thus this procedure introduces an error by the use of the weak-inverse. The error is therefore

$$\mathbf{v} - \mathbf{v} = (\mathbf{H}_n^2 - \mathbf{I}_n) \mathbf{v}. \quad (10)$$

As we see, the error $\mathbf{v} - \mathbf{v}$ depends on $\mathbf{H}_n^2 - \mathbf{I}_n$, as well as on the original message \mathbf{v} .

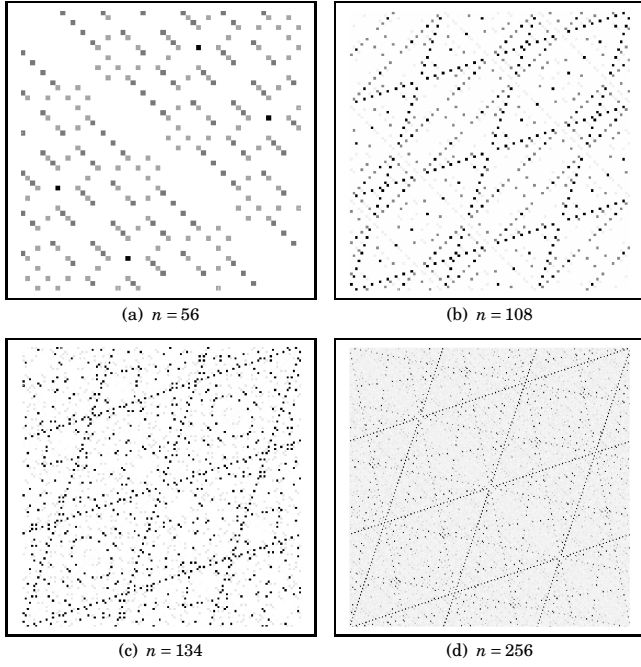


Figure 6: Some interesting pictorial matrix patterns for \mathbf{H}_n^2 , $n = 56, 108, 134$ and 256 . A gray scale is used to plot the intensity of the elements: the darker the element, the greater its magnitude (white denotes zeroes). Main diagonal omitted for better visualization, since the magnitude of the diagonal elements is much greater than the other elements’.

3.3.2 Fractal

Since the measure $\bar{\mu}(\mathbf{H}_n^2 - \mathbf{I}_n)$ presents a fractional exponent (Equation 8), objects $\mathbf{H}_n^2 - \mathbf{I}_n$ should be associated with some fractal. The patterns displayed in Figure 6 show a kind of self-similar behavior, as expected.

4 A Fast Algorithm for RHT

In order to derive a fast algorithm, we use a naive example: 16-point RHT, which transform matrix \mathbf{H}_{16} is shown below:

$$\mathbf{H}_{16} = \begin{pmatrix} 1 & 1 & 1 & 1 & 1 & 1 & 1 & 1 & 1 & 1 & 1 & 1 & 1 & 1 & 1 & 1 \\ 1 & 1 & 1 & 1 & 1 & 1 & 1 & 1 & 1 & 1 & 1 & 1 & 1 & 1 & 1 & 1 \\ 1 & 1 & 1 & - & - & - & 1 & 1 & 1 & - & - & - & - & - & - & - \\ 1 & 1 & - & 1 & 1 & - & - & - & 1 & 1 & - & - & - & - & - & - \\ 1 & 1 & - & 1 & 1 & - & - & 1 & 1 & - & - & 1 & 1 & - & - & - \\ 1 & 1 & - & 1 & - & 1 & - & - & 1 & - & - & 1 & - & - & 1 & - \\ 1 & 1 & - & 1 & - & 1 & - & 1 & - & 1 & - & 1 & - & 1 & - & 1 \\ 1 & 1 & - & 1 & - & 1 & - & 1 & - & 1 & - & 1 & - & 1 & - & 1 \\ 1 & 1 & - & 1 & - & 1 & - & 1 & - & 1 & - & 1 & - & 1 & - & 1 \\ 1 & 1 & - & 1 & - & 1 & - & 1 & - & 1 & - & 1 & - & 1 & - & 1 \\ 1 & 1 & - & 1 & - & 1 & - & 1 & - & 1 & - & 1 & - & 1 & - & 1 \\ 1 & 1 & - & 1 & - & 1 & - & 1 & - & 1 & - & 1 & - & 1 & - & 1 \\ 1 & 1 & - & 1 & - & 1 & - & 1 & - & 1 & - & 1 & - & 1 & - & 1 \\ 1 & 1 & - & 1 & - & 1 & - & 1 & - & 1 & - & 1 & - & 1 & - & 1 \\ 1 & 1 & - & 1 & - & 1 & - & 1 & - & 1 & - & 1 & - & 1 & - & 1 \end{pmatrix},$$

where “-” represents -1 and blank spaces are zeroes.

Using methods described in [7], we obtained the implementation diagram displayed in Figure 7.

The algorithm turns out to have embedding properties: shorter transforms are found in major ones. In the 16-point RHT, the following transforms are embedded: 2-, 4- and 8-point RHT. By zeroing some inputs, a shorter transform is promptly available (e.g. let $v_8 = \dots = v_{15} = 0$ to have an 8-point RHT). This feature makes the algorithm particularly flexible to a much larger range of applicabilities [2, 7].

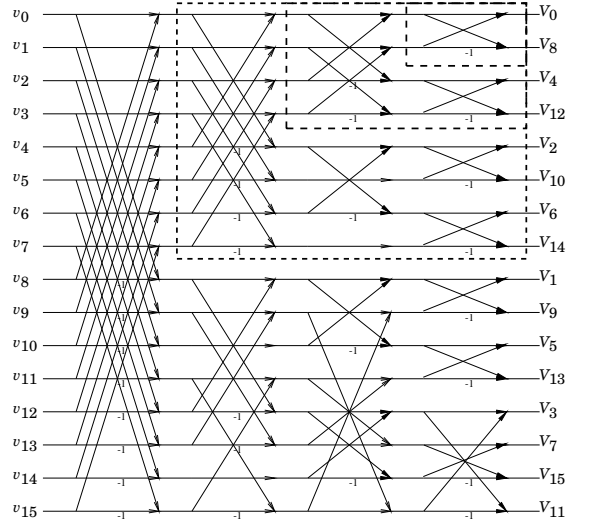


Figure 7: Flow graph for the fast algorithm of 16-point rounded Hartley transform. Note the complete absence of multipliers. The dashed boxes denote shorter transforms embedded in 16-point RHT.

For blocklengths which are power of two, one can find out the the following arithmetic complexity:

$$A(n) = \mathcal{O}(n \log_2 n), \quad (11)$$

$$M(n) = 0, \quad (12)$$

where $\mathcal{O}(\cdot)$ is the Landau symbol.

5 2-D Rounded Hartley Transform

Original two-dimensional Hartley transform of an $n \times n$ image is defined by

$$b_{u,v} = \sum_{i=0}^{n-1} \sum_{j=0}^{n-1} a_{i,j} \cdot \text{cas}\left(\frac{ui+vj}{n}\right), \quad (13)$$

where $a_{i,j}$ are the elements of an image \mathbf{A} and $b_{u,v}$ are the elements of the Hartley transform of \mathbf{A} .

Since $\text{cas}(\cdot)$ kernel is not separable, we cannot express the two-dimensional transform in terms of a single matrix equation, like the 2-D discrete Fourier transform. Thus, we defined the two-dimensional rounded Hartley transform similarly to Bracewell’s method for two-dimensional discrete Hartley transform [3].

Let \mathbf{A} be the $n \times n$ image matrix. We start the procedure by calculating a temporary matrix \mathbf{T} , as follows:

$$\mathbf{T} = \mathbf{H}_n \cdot \mathbf{A} \cdot \mathbf{H}_n, \quad (14)$$

where \mathbf{H}_n is the rounded Hartley matrix of order n . This is equivalent to take one-dimensional Hartley transform of the rows, and then transform the columns [9].

Establishing that the elements of \mathbf{T} are represented on the form $t_{i,j}$, $i, j = 0, \dots, n-1$, we can consider three new matrices built from the temporary matrix \mathbf{T} : $\mathbf{T}^{(c)}$, $\mathbf{T}^{(r)}$ and $\mathbf{T}^{(cr)}$ which elements are $t_{i,n-j \pmod n}$, $t_{n-i \pmod n, j}$, $t_{n-i \pmod n, n-j \pmod n}$, respectively. These different indexes flip matrix \mathbf{T} in left-right direction, except from the first column ($\mathbf{T}^{(c)}$); in up-down direction, except from the first line ($\mathbf{T}^{(r)}$); and both operations at same time ($\mathbf{T}^{(cr)}$).

Using these constructs, the rounded Hartley transform \mathbf{B} of an $n \times n$ image \mathbf{A} is defined as

$$\mathbf{B} \triangleq \mathbf{T} + \mathbf{T}^{(c)} + \mathbf{T}^{(l)} - \mathbf{T}^{(cl)}. \quad (15)$$

Table 1: PSNR of some standard images after a direct and weak-inverse rounded Hartley transform. All images were obtained from USC-SIPI Image Database. In parenthesis, image ID number.

Image	Dimension (pixels)	PSNR (dB)
Moon surface (5.1.09)	256 × 256	26.5522
Airplane (5.1.11)	256 × 256	25.7277
Aerial (5.2.09)	512 × 512	22.2006
APC (7.1.08)	512 × 512	27.3035
Tank (7.1.09)	512 × 512	24.4590

This definition derives directly from the $\text{cas}(\cdot)$ property: $\text{cas}(a + b) = \text{cas}(a)\text{cas}(b) + \text{cas}(a)\text{cas}(-b) + \text{cas}(-a)\text{cas}(b) - \text{cas}(-a)\text{cas}(-b)$.

Program 1 A simple MATLAB program to compute 2-D RHT, its weak-inverse and the PSNR.

```
function Z = rcas(N)

i = 0:(N-1);
j = 0:(N-1);
[I,J] = meshgrid(i,j);
Z = round ( cas ( 2 * pi / N * I .* J ) );

function [B, AA, PSNR] = twodrht(file)

A = imread(file, 'bmp');
A = double(A);
[M, N] = size(A);
if M ~= N end;
colormap(gray(256));
K = rcas(N);
TEMP = K * A * K;
TEMPFLIPCOL = [TEMP(:,1),fliplr(TEMP(:,2:N))];
TEMPFLIPROW = [TEMP(1,:),flipud(TEMP(2:N,:))];
TEMPFLIPRC = [TEMPFLIPCOL(1,:);flipud(TEMPFLIPCOL(2:N,:))];
B = (1/2)*(TEMP+TEMPFLIPCOL+TEMPFLIPROW-TEMPFLIPRC);
temp = (1/N) * (1/N) * K * B * K;
tempFLIPCOL = [temp(:,1),fliplr(temp(:,2:N))];
tempFLIPROW = [temp(1,:),flipud(temp(2:N,:))];
tempFLIPRC = [tempFLIPCOL(1,:);flipud(tempFLIPCOL(2:N,:))];
AA = (1/2)*(temp+tempFLIPCOL+tempFLIPROW-tempFLIPRC);
MSE = (1/N^2) * sum(sum((AA-A).^2));
RMSE = sqrt(MSE);
PSNR = 20 * log10(255/RMSE);
```

Aiming to investigate such degradation (which follows from the use of weak-inverse), standard images from Signal and Image Processing Institute Image Database [14] at University of Southern California were analyzed. Figures 8 and 9 present original images and their respective recovered images using the weak-inverse transform instead of the (exact) inverse transform. Program 1 lists a naive implementation of 2-D RHT using MATLAB.

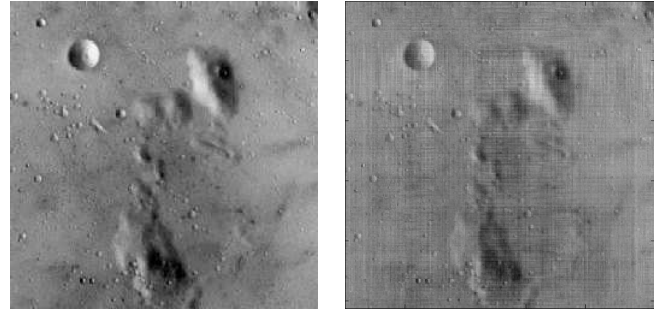
Table 1 brings PSNR (Peak Signal-Noise Ratio) of the standard images after a direct RHT and a weak-inverse RHT. Observe that the PSNR is image dependent: the quantization noise due to the rounding depends on the original image characteristics, such as shape, contrast, dimension etc.

6 Connection with Fourier and Walsh/Hadamard Transform

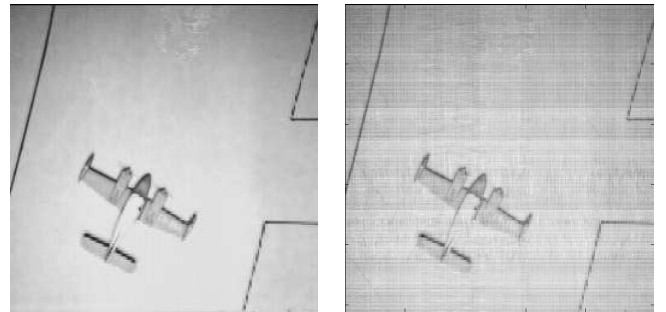
As final comments on RHT, we present some relationship between this new transform and other well-known transforms such as Fourier and Walsh/Hadamard transforms.

Since DHT can be used to compute de DFT [2], and the RHT furnishes a estimate for DHT, we can use RHT to derive a rough — but fast — evaluation of Fourier spectrum.

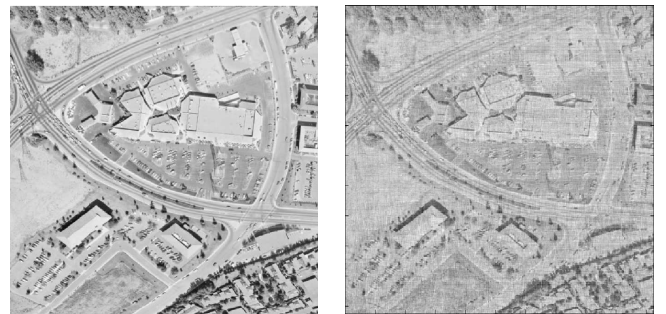
de Oliveira and co-workers [6] found a relationship between discrete Hartley transform and Hadamard transform. Such link was



(a) Moon surface



(b) Airplane



(c) Aerial

Figure 8: Direct and Weak-inverse Transform. The original pictures displayed on left were direct and weak-inverse transformed via the rounded Hartley transform. Resulting images are seen on the right. Since RHT is a quasi-involution, it introduces noise due to its nature.

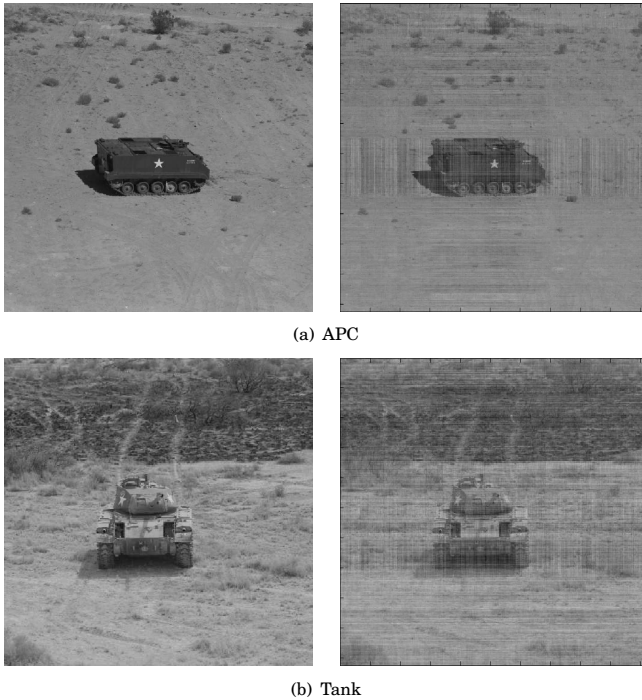


Figure 9: Direct and Weak-inverse Transform. Military images.

exploited to derive new fast algorithms [4, 6, 7]. In the present framework, we are led to following conjecture:

Conjecture 2 *Let n be a power of 2. The matrix \mathbf{H}_n is identical to Walsh/Hadamard matrix of same order, except for null elements and for a permutation of columns.* \square

For example, the column permutation that, except for zero elements, converts an 8-point rounded Hartley matrix into a Walsh transformation is (4 8) (cyclic notation).

7 Conclusions

Discrete Hartley transform has long been used in practical applications. It is real-valued self-inverse transform, more symmetrical than the DFT [2].

A new multiplication-free transform derived from DHT is introduced, the RHT, which kept many properties of discrete Hartley transform. In spite of not being involutorial, it is shown that RHT exhibits quasi-involutorial property, a new concept derived from the periodicity of matrices.

The quasi-involutorial property was induced from weak-inverse definition. Instead of using the (true) inverse transform, the RHT is viewed as an involutorial transform, allowing the use of direct (multiplication-free) to evaluate the inverse. Thus, the software/hardware to be used in the computation of both the direct and the inverse RHT becomes exactly the same. The price to be paid by not using the exact inverse transform is some degradation when recovering original signal.

Fast algorithms to compute RHT are presented showing embedded properties. The 2-D RHT is also defined, allowing to analyze the effects of this approach on standard images. Despite of SNR loss, RHT can be very interesting for applications involving image monitoring associated to decision making, such as military applications or medical imaging.

RHT is offered as an efficient way to compute real-time initial estimations of spectral evaluations. Refinement algorithms can be used to improve the image or spectral estimation, when necessary. A class of refinement algorithms for this particularly transform is now our object of investigation.

References

- [1] N. BHATNAGAR, *A binary friendly algorithm for computing discrete Hartley transform*, DSP'97, (1997), pp. 353–356.
- [2] R. N. BRACEWELL, *The Hartley Transform*, Oxford, 1986.
- [3] R. N. BRACEWELL, O. BUNEMAN, H. HAO, AND J. D. VILLASENOR, *Fast two-dimensional Hartley transform*, Proceedings of IEEE, 74 (1986), pp. 1282–1283.
- [4] R. J. CINTRA, H. M. DE OLIVEIRA, AND R. M. CAMPELLO DE SOUZA, *Um algoritmo bifuncional para a avaliação dos espectros de Hadamard e Hartley*, in XIX Simpósio Brasileiro de Telecomunicações, Fortaleza, Brazil, Sept. 2001.
- [5] R. J. CINTRA AND H. M. DE OLIVEIRA, *How to interpolate in arithmetic transform algorithms*, in IEEE 27th International Conference on Acoustics, Speech, and Signal Processing, Orlando, U.S.A., May 2002.
- [6] H. M. DE OLIVEIRA, R. J. CINTRA, AND R. M. CAMPELLO DE SOUZA, *The multilayer Hadamard decomposition of the discrete Hartley transform*, in XVIII Simpósio Brasileiro de Telecomunicações, Gramado, Brazil, Sept. 2000.
- [7] ———, *A factorization scheme for some discrete Hartley transform matrices*, in ICSECT 2001 Proceedings – International Conference on System Engineering, Communications and Informations Technologies, Universidad de Magallanes, Punta Arenas, Chile, 2001.
- [8] H. S. DEE AND V. JEOTI, *Computing DFT using approximate fast Hartley transform*, International Symposium on Signal Processing and its Applications (ISSPA), (2001), pp. 100–103.
- [9] R. C. GONZALEZ AND R. E. WOODS, *Digital Imaging Processing*, Addison-Wesley, 1992.
- [10] M. T. HEIDEMAN, *Multiplicative Complexity, Convolution, and the DFT*, Springer-Verlag, 1988.
- [11] K. J. OLEJNICZAK AND G. T. HEYDT, *Scanning the special section on the Hartley transform*, Proceedings of the IEEE, 82 (1994), pp. 372–380.
- [12] C. H. H. PAIK AND M. D. FOX, *Fast Hartley transforms for image processing*, IEEE Transactions on Medical Imaging, 7 (1988), pp. 147–153.
- [13] I. S. REED, D. W. TUFTS, X. YU, T. TRUONG, M.-T. SHIH, AND X. YIN, *Fourier analysis and signal processing by use of the Möbius inversion formula*, IEEE Transactions on Acoustics, Speech, and Signal Processing, 38 (1990), pp. 459–470.
- [14] *The USC-SIPI image database*. <http://sipi.usc.edu/database/>. University of Southern California, Signal and Image Processing Institute.